Accuracy of a Novel Virtual Articulator for Recording Three-Dimensional Dentition

7 authors, including:

Ning Dai
Massachusetts General Hospital
105 PUBLICATIONS **1,072** CITATIONS

SEE PROFILE

Sukun Tian
Nanjing University of Aeronautics & Astronautics
9 PUBLICATIONS **10** CITATIONS

SEE PROFILE

Some of the authors of this publication are also working on these related projects:

Project   Biomedical Engineering View project

Accuracy of a Novel Virtual Articulator for Recording Three-Dimensional Dentition

Linlin Li, PhD
Yuchun Sun,* DDS, PhD
Yong Wang,* Professorate Senior Engineer

*Center of Digital Dentistry, Peking University School and Hospital of Stomatology;
National Engineering Laboratory for Digital and Material Technology of Stomatology;
Research Center of Engineering and Technology for Digital Dentistry of Ministry of Health;
Beijing Key Laboratory of Digital Stomatology; National Clinical Research Center for Oral Diseases,
Beijing, China.*

Weiwei Li, PhD

Department of Prosthodontics, Peking University School and Hospital of Stomatology, Beijing, China.

Ning Dai, PhD
Sukun Tian, ME
Haihua Cui, PhD

*College of Mechanical and Electrical Engineering, Nanjing University of Aeronautics and Astronautics,
Nanjing, China.*

These authors contributed equally to this work.

Purpose: To research and develop a novel virtual articulator system (the PN-300) based on computer binocular vision, raster scanning, and simulation technology and to conduct a preliminary evaluation of its accuracy. **Materials and Methods:** Two digital cameras were used to build the trajectory-tracking part of the virtual articulator system, and cameras combined with a projection module were used to form the scanning part of the system. The most prominent feature of the PN-300 is its ability to simultaneously obtain the 3D data of the subject's teeth and the movement trajectory of the mandible relative to the maxilla. The PN-300 recorded the linear, circular, and rectangular quadrilateral movements of a high-accuracy 3D electronic translation stage. The accuracy of measurement of the inclination of incisal guidance derived from the PN-300 based on the PROTAR evo7 articulator was also estimated. **Results:** The measurement error was below 100 µm for the linear and circular movements, and the angle error was within 0.2 degrees for the rectangular quadrilateral movements. The error of inclination of protrusive incisal guidance was 1.51 ± 0.68 degrees, and for incisal guidance was 0.82 ± 0.55 degrees. Trajectories and incisal 3D data obtained by the PN-300 were combined with data from plaster models and CBCT to simulate mandibular movement and to calculate the trajectories of the condyle. **Conclusion:** The PN-300 achieved a good accuracy for recording mandibular movement and can be expected to calculate the movement of the condyle. *Int J Prosthodont 2020;33:441–451. doi: 10.11607/ijp.6480*

The human mandible and the temporomandibular joints (TMJs) compose a complex biomechanical system that performs several functions, including chewing, swallowing, and pronunciation. Studying mandibular movement promotes the understanding of normal function of the TMJ and has a profound impact on the etiology, diagnosis, and subsequent treatment of TMJ disorders.[1–3] In addition, the study of mandibular movement can also be used to assess the state of the masticatory muscles,[4,5] as well as assist physicians in defining adequate treatment plans to address the occlusion problem.[6] It can also be used to evaluate the impact of systemic disease on the stomatognathic system.[7] Therefore, the study of mandibular movement is a topic of great importance in current dental practice.[6,8]

Physical dental articulators are tools that simulate the movements of the human mandible and the TMJs. Physical dental articulators enable technicians to study the occlusal relations between dental arches and to detect harmful occlusal interferences

on models. Using a mechanical facebow, the relationship between the maxilla and the TMJs is transferred from the patient onto the mechanical dental articulator. With the advancement of digital dental technology, virtual articulators (VAs) have gradually replaced mechanical articulators. VAs dynamically simulate mandibular movement, visualize the occlusal contacts, and simulate movement that a mechanical articulator cannot provide, such as the Bennett movement. The application of this technology gives clinicians more selectivity and allows for more personalized restorations.[9,10] In addition, when compared to mechanical articulators, VAs have high precision and study mandibular movement at a specific time, consequently enhancing diagnosis and treatment as well as reducing operating time.[11–13] VAs are divided into those based on mathematical simulation of existing mechanical articulators and those designed to move digitized dental arches along these individual movement paths on the computer.[14,15]

In order to enable VAs to accurately simulate mandibular movement, the movement of the mandible relative to the maxilla must be obtained. Currently, there are many kinds of mandibular movement–recording devices. These devices are mainly divided into optoelectronic jaw movement recording systems, electromyographic instruments (CADIAX [Whip Mix],[16] K6-I [Myotronics][17]), electromagnetic tracking devices (mandibular kinesiograph [MKG], electromagnetic articulograph [EMA],[8] FASTRAK [3Space][18]), ultrasonic motion capture devices (ARCUSdigma [KaVo],[19] zebris jaw motion analysis [JMA][20–23]), and imaging methods (computed tomography [CT], magnetic resonance imaging [MRI][24–27]). The measuring devices for electromyographic, electromagnetic, and ultrasonic recording methods require fixing the measuring device on the mandible and cranium. However, when the equipment is fixed directly on the soft tissue of the head, the instability of the soft tissue will affect the accuracy of the mandibular movement recording, and these devices will also interfere with normal mandibular movement when fixed on the mandible.[2] Devices based on electromyographic, electromagnetic, and ultrasonic technology are always expensive and complex.[5,28,29] Electromagnetic systems may pose risks for patients using some medical devices, and external magnetic fields and large metal objects may interfere with recording sessions.[18] In addition, these systems can only record the trajectory of mandibular movement without obtaining the three-dimensional (3D) data of the dentition at the same time; so, additional steps are needed to determine the spatial-positional relationship between the trajectory data and the 3D dentition data, resulting in increased sources of error.

Previous studies have evaluated the accuracies of various systems. Pinheiro et al[5] utilized a single charge-coupled device (CCD) camera and a reflective marker fixed to the mandible to record mandibular movements in a two-dimensional space, with a mean error of 0.4 mm in the frontal and sagittal planes. Fang and Kuo[30] presented a system composed of a pair of CCD cameras and three light-emitting diodes (LEDs) affixed to a pair of tracking plates for 3D reconstruction and found that root mean square (RMS) accuracy was 0.198 mm. Another optoelectronic recording system reported by Furtado et al[28] consisting of three infrared cameras and a set of reflective markers presented a mean error of 0.156 mm and a precision of 0.259 mm within the volume intended for recording mandibular movement. An imaging system described by Chen et al[2] using single-plane fluoroscopy images and 3D low-radiation cone beam CT (CBCT) data to measure the 3D motion of the mandible in vivo demonstrated measurement errors less than 1.0 ± 1.4 mm for all translations and 0.2 ± 0.7 degrees for all rotations. Baltali et al[18] combined motion recordings from an electromagnetic tracking device with 3D CT images to track the motion changes of the TMJ. The accuracy of the linear distance calculations was 0.027 ± 0.129 mm, and of the curvilinear path calculations was 0.360 ± 0.438 mm.

To solve these problems, the present authors proposed a fast, high-precision, low-cost virtual articulator system based on computer binocular vision, raster scanning, and simulation technology—the PN-300—and conducted a preliminary laboratory evaluation of its accuracy. Zhao et al[29] performed an initial laboratory evaluation, but the first-generation system could only record single-jaw movement. Functions were added based on this first system to form the present system. This new system can record the movements of the targets representing mandibular and maxillary movements in real time and acquire the 3D data of the dentition in the same coordinate system as the trajectory data at the same time. Then, the trajectory data and 3D data of the dentition can be imported into a simulation program to achieve individualized simulation of mandibular movement. The whole protocol for recording and evaluating accuracy is shown in Fig 1.

MATERIALS AND METHODS

Recording of 3D Dentition and Target Trajectories

The premise of simulating personalized mandibular movement is to obtain the spatial relationship between trajectory and anatomy. In order to achieve this, the device consisted of two digital cameras (The Imaging Source Europe) and a projection module (Texas Instruments) (Fig 2). The projection module was mounted equidistantly between the two cameras, which were at the same angle with the sagittal plane.

Before the system works, the cameras need to be calibrated. Through calibration, the relationship between
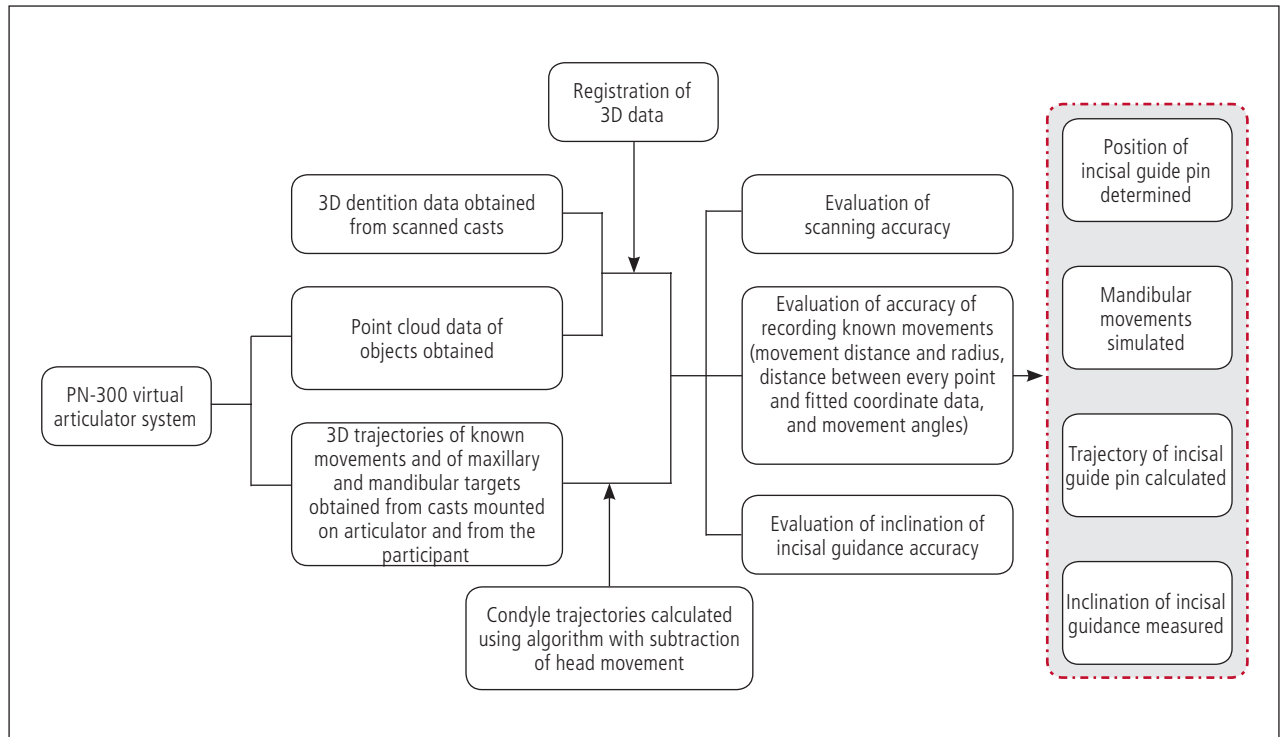
Fig 1 Flowchart of study protocol.

the two-dimensional (2D) image coordinates and the 3D world coordinates[28] can be determined, and the trajectory tracking module and scanning module could be integrated in the same coordinate system. The system used the Zhang Zhengyou plane template method[31] for calibration since it is relatively simple and provides good precision, with an error of about 10 μm. The technique required the cameras to observe a planar calibration board (Nanjing Gaoxi Electronic Technology) shown in 11 different orientations.[31]

Acquisition of 3D Point Cloud Data for Test Objects

In order to compute exact mandibular movements, it is essential to obtain the geometrical relationship between the trajectory and anatomical structures.[32] Therefore, the PN-300 virtual articulator system consisted of two modules: a track acquisition module and a module for acquisition of 3D data of the dentition. The PN-300 scanned the dentition, obtained the 3D point cloud data, and stored the point cloud data in TXT format. The 3D reconstruction was then carried out, and triangulation of the point cloud data obtained was performed using Geomagic Studio 2013 software (3D Systems). Geomagic software is used to process 3D data and can achieve triangulation of point cloud data well. The present authors will also develop their own software package to implement such functions.
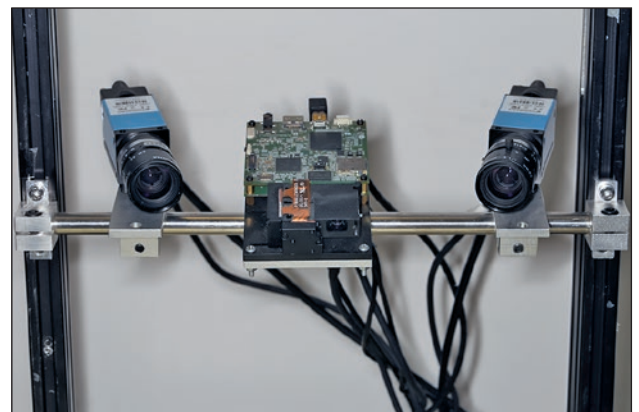
Fig 2 Overall structure of the PN-300 virtual articulator system.

Center Recognition, Tracking, and the Output of Relative Position

The targets (Nanjing Gaoxi Electronic Technology) used by the system were characterized by concentric circles. The targets have inverted colors to distinguish between maxillary and mandibular movements (Fig 2). Using black as a background can facilitate target recognition during tracing with the digital video cameras. The cameras took time-series pictures of the targets with a sampling rate of 120 Hz and calculated the coordinates
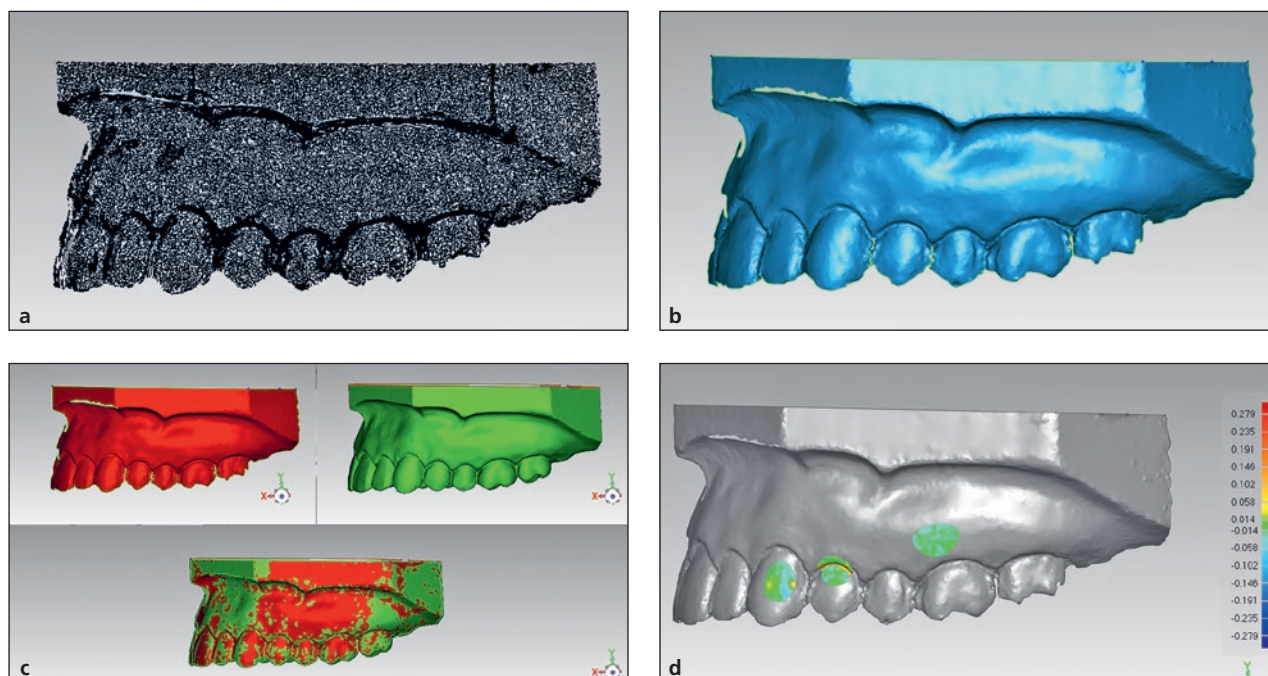
Fig 3 3D analysis of deviation. *(a)* 3D scan of left maxillary plaster cast with PN-300. *(b)* 3D reconstruction of maxillary cast with Geomagic software. *(c)* Registration of data from the PN-300 and model scanner. *(d)* Three areas were chosen for analyzing the point cloud deviation to analyze the scanning accuracy of the PN-300.

of each target's center to record its movement. The center-of-circle recognition was divided into four steps. The first step was to filter the left and right camera images to reduce noise.[33] The position of the target was extracted as a contour based on the brightness of each image using the Canny edge detection method.[34] However, since the circular target tends to transform into an ellipse[33] in the perspective projection transformation, the actually detected edge is mostly elliptical. Next, the ellipse was fitted using the processed respective edge data. Last, the centroid method[33] was used to extract the center of the ellipse.

By tracking the target centers, the system could record the trajectories of the upper and lower targets, representing the maxilla and mandible, respectively. Taking the coordinates of the initial position of the maxillary target $F = (F_x, F_y, F_z)$ as a reference, the coordinates of the other positions, except for the initial position of the maxillary target, $S = (S_x, S_y, S_z)$, were transformed into the initial position using matrix transformation. The generated matrix acted on the coordinates of the mandibular target to obtain the coordinates of that target relative to the maxillary target. In this way, the relative movement of the target fixed on the mandible was available, with subtraction of any head movement. For more details, please refer to the previous article by the present research group.[35]

Preliminary Evaluation of System Accuracy
The accuracy of any simulation will be affected by dentition scanning error and trajectory error. The accuracies of these two kinds of data are evaluated separately here. An electronic translation stage (Beijing stand upright, Han Optical Instruments, with an accuracy of 0.001 mm) was used to simulate known movements, and the PN-300 recorded these movements to evaluate the accuracy of recording simple movements. In addition, the PN-300 was used to scan the standard casts mounted on the articulator and to record the movements of the maxillary and mandibular casts to analyze the accuracy of recording 3D dentition data and mandibular movement.

Evaluation of PN-300 Scanning Accuracy
The 3D laser dental model scanner (Activity 880, Smart Optics, with an accuracy of 0.010 mm) was used to scan the standard maxillary plaster cast three times and obtain the 3D data in standard triangulation language (STL) format. The data with the least number of replenishments and no holes were selected as the gold standard. The PN-300 was used to scan the same cast five times to obtain the point cloud data of the left maxillary plaster cast (Fig 3a). 3D reconstruction of the point cloud data and registration of the data were performed with Geomagic Studio 2013 software (Figs 3b and 3c).

Three areas were chosen for analyzing the point cloud deviation with the 3D deviation analysis tool. The deviation was used to analyze the scanning accuracy of the PN-300 (Fig 3d). In Fig 3, it can be seen that the deviations were smaller in the area of the buccal surface of the crown and the soft tissue area and greater in the gingival margin area.

Accuracy of Recording Known Movements

An electronic triaxial translation stage was used to carry out linear movements in three axes (x, y, and z), and circular and rectangular quadrilateral movements in three planes (xoy, xoz, and yoz). The target consisted of three pairs of concentric circles, and the centers of the circles constitute an isosceles right triange. The right angle vertext of the triangle is defined as "b," the vertex perpendicular to "b" is defined as "a," and the third point as "c." Every movement was repeated five times with a velocity of 1 mm/second, and the PN-300 recorded the movements. The movement distance was 10 mm, and the radius was 5 mm. The same type of movement was done in 1 day, and all types of movements were carried out at the same temperature of 22°C with incandescent light intensity. Referring to Zhao et al[29] and Tian et al,[35] the movement distance and radius, the distance between every point and the fitted lines and circles, and the angles of the movements were calculated using Imageware 13 software (Siemens PLM) (Fig 4).

Evaluating Accuracy of Inclination of Incisal Guidance

The standard casts with targets were mounted on the PROTARevo7 articulator (KaVo) (Fig 5a). The maxillary cast had no occlusal contact with the mandibular cast in order to avoid the influence of intercuspal occlusion on the articulator movement. Then, the FaroArm Edge 7-Axis contact measurement system (FARO Technologies; contact measurement accuracy of 0.024 mm and a scanning accuracy of 0.059 mm) was used to scan the plaster casts mounted on the articulator with the scanning function and to measure the sphere on the top of the incisal guide pin, the base plane of the articulator, and the bilateral condylar spheres using the contact measurement function. The data obtained by the two functions were in the same coordinate system (Fig 5b). Next, the inclination of laterotrusive incisal guidance was set to 0, 10, 20, 30, and 40 degrees, and the right laterotrusive movement (left lateral movement of the maxillary cast) was simulated. The inclination of protrusive incisal guidance was set to the same measures, and protrusive movement (retruding movement of the maxillary cast) was simulated. After each set of parameters, the PN-300 was used to scan the casts and then to record the movements of the casts through the targets (Fig 5c). Every movement
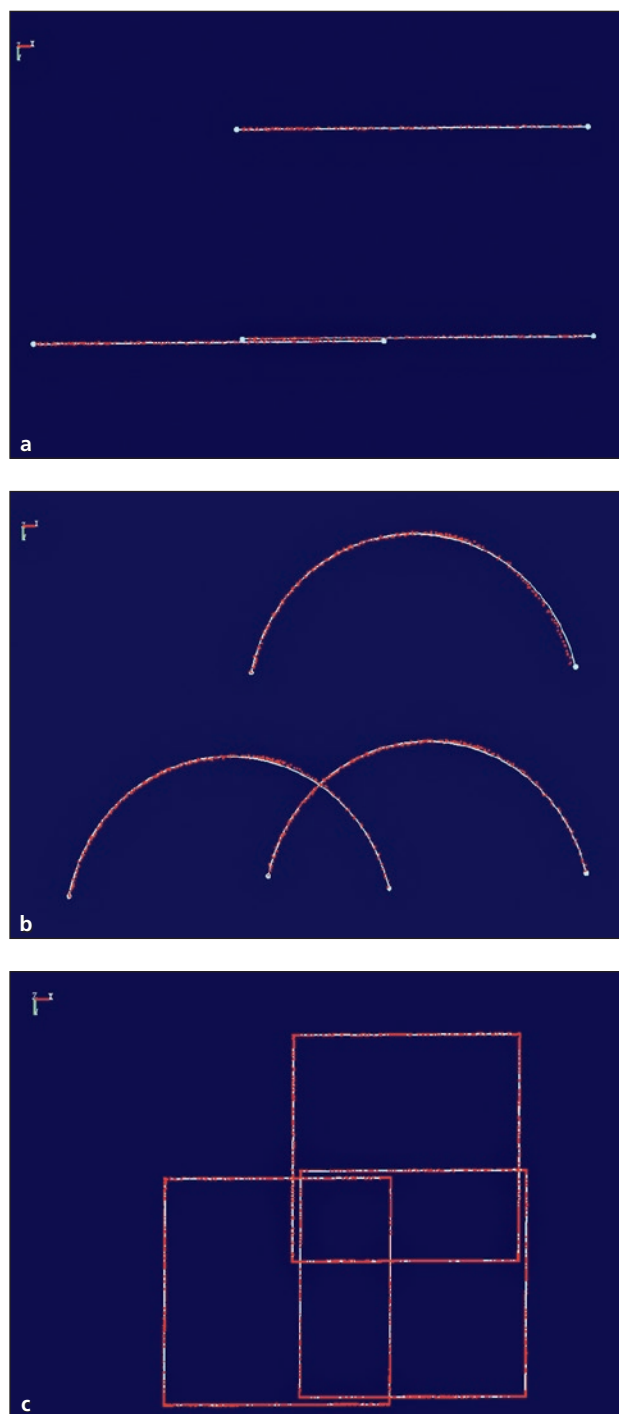
Fig 4 Deviation analyses of known movement trajectories for *(a)* linear, *(b)* circular, and *(c)* quadrilateral movements.

was repeated 10 times and finished in 1 day under the same environmental conditions mentioned above. Because the PN-300 could only scan part of the arch, complete arch cast data were registered and obtained using a model scanner in the PN-300 coordinate system
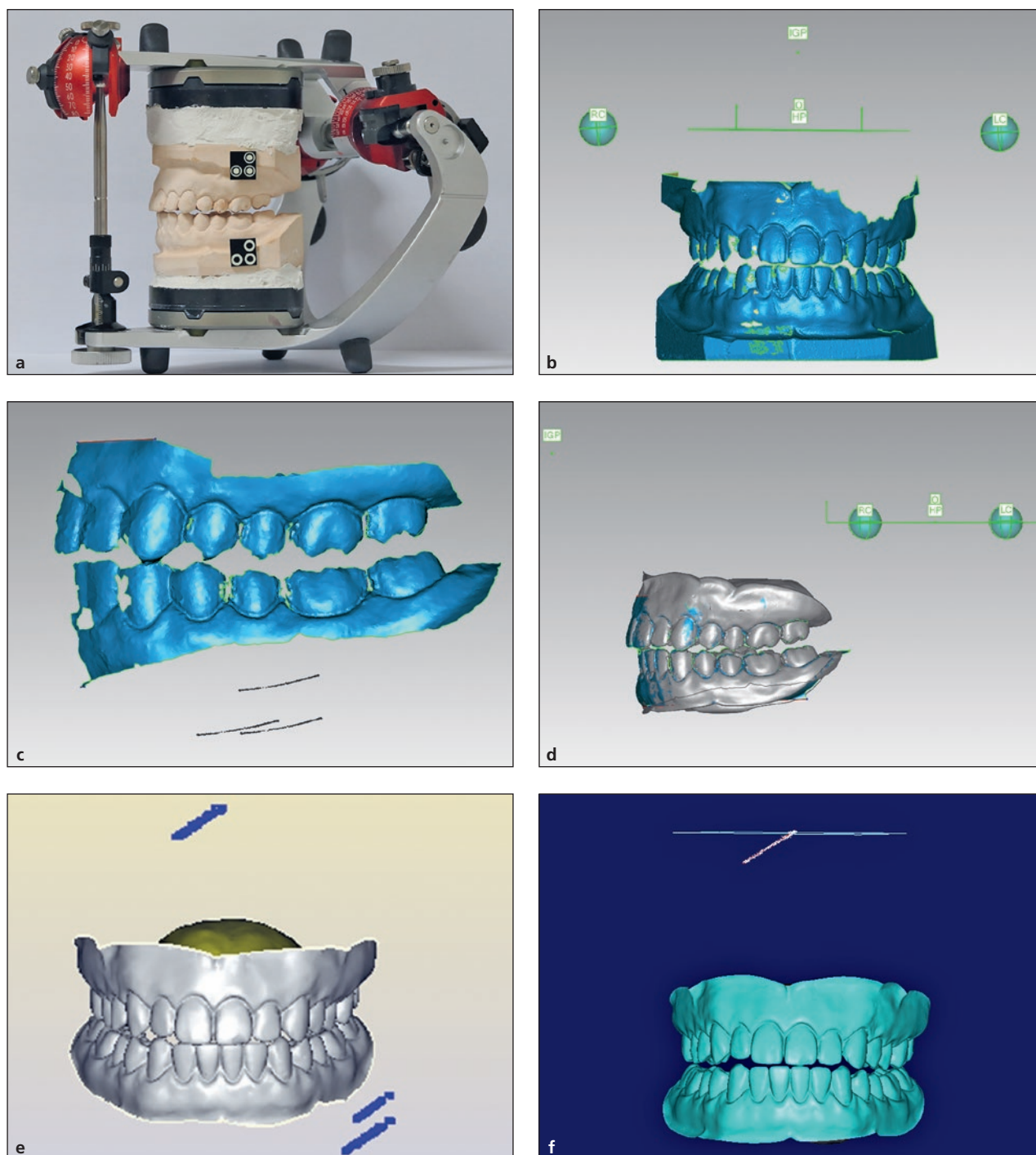
Fig 5 Process of deriving the inclination of incisal guidance. *(a)* Standard casts mounted on articulator. *(b, c)* 3D data obtained by the FaroArm Edge, PN-300, and model scanner, respectively. *(d)* Registration of 3D data. *(e) T*rajectory of incisal guide pin. *(f)* Inclination of incisal guidance. IGP = center of the sphere at the top of the incisal guide pin; RC = right condylar sphere; LC = left condylar sphere; HP = horizontal plane; O = original point.

to replace the partial arch data obtained by the PN-300 (Fig 5d). The point cloud data of casts obtained by the FaroArm system and the PN-300 and model scanner were imported into Geomagic Studio 2013 to accept the 3D reconstructions, and then the two 3D datasets were manually registered to achieve coordinate transformation of the FaroArm coordinate system (Fig 5d). The center of the sphere at the top of the incisal guide pin and the base plane of the articulator in the PN-300 coordinate system were exported.
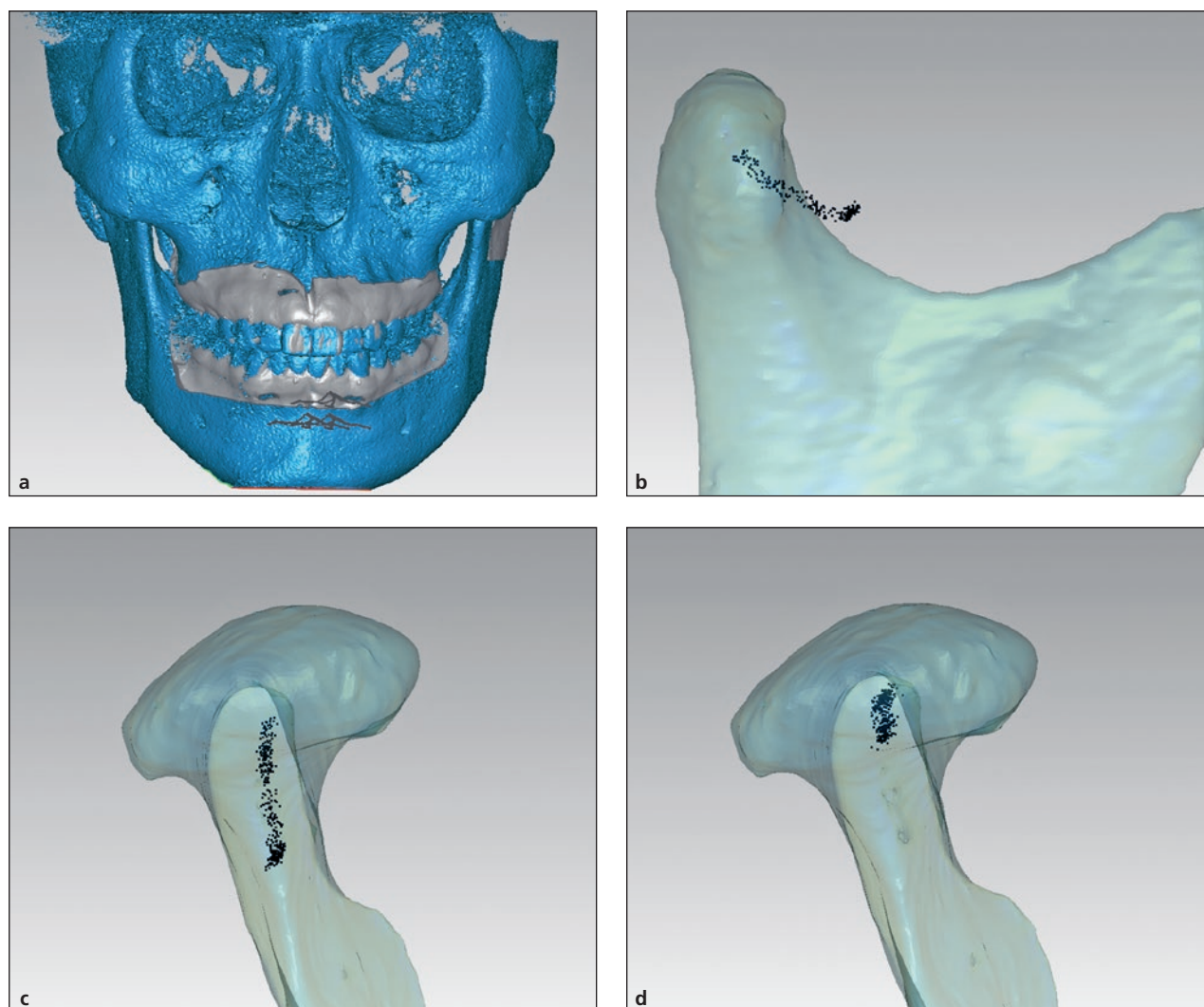
Fig 6 Workflow for calculating the condyle trajectories. *(a)* Registration of trajectories, 3D data of casts, and arches. *(b)* Protrusive movement trajectory of the condyle and trajectories of *(c)* nonworking and *(d)* working sides.

The 3D data of complete-arch casts, the movement trajectories of both targets, and the coordinates of the center of the sphere at the top of the incisal guide pin, which were all in the same coordinates, were imported into the self-developed virtual simulation program to achieve reconstruction of mandibular movement and to assess the trajectory of the center of the sphere at the top of the incisal guide pin (Fig 5e). The trajectory obtained by the simulation system was fitted to straight lines, and then the angles with the base plane of the articulator were measured using Imageware 13 software (Fig 5f).

Calculating the Condyle Trajectories

This research was approved by the Bioethics Committee of Peking University School and the Hospital of Stomatology, PR China. Written informed consent was obtained from the participant.

The subject's mandibular movements were recorded, and the trajectories of the condyles (with complete permanent dentition with the occlusal surfaces intact, without carious lesions, abrasions, attrition, erosion, or any sign of temporomandibular disorders) were calculated. Alginate impressions (Kulzer) of both arches were made, and stone replicas of Type V dental stone (Pemaco) were fabricated. The occlusal surfaces of the models and the buccal images in intercuspal position (ICP) were scanned after 24 hours with a dental model scanner and saved in STL format (Fig 6). The digital impressions were imported into Geomagic, and the buccal areas of the incisors and premolars were selected. An offset (0.1 mm) was used to generate a new shell from the selected area and extrude

it to 1.5 mm. The so-designed splints, which followed the individual teeth, were smoothed and, when necessary, reinforced by means of sculpting tools. The buccal side extended a handle like an individual tray handle on which to stick the targets. The thus-generated object was prepared for printing using polylactic acid (PLA) material and a 3D printer (Shino Technology, with its xy axis positioning accuracy of 10 μm and its z axis positioning accuracy of 5 μm).

Moisture was reduced by dabbing the teeth with a cotton roll. Autopolymerizing composite Luxatemp (DMG) was applied to the bending parts of the splints and adapted to the tooth surfaces. Excess material and sharp edges were removed to guarantee an undisturbed functional movement of the jaw in occlusion. Washable matte opacifier (YETI Dental) was used to spray the tooth surfaces to minimize scanning errors of teeth with high gloss. Then the subject was guided to do protrusive and laterotrusive movements one time, and the PN-300 recorded the 3D point cloud data of the anterior teeth as well as the movements. This process was repeated three times, with intervals of 30 minutes between procedures. The trajectory with the most uniform point distribution was chosen to derive the trajectory of the condyle. The segmentation and 3D reconstruction of the skull and arches were performed using CBCT data in Materialise Mimics 17.0 software. Digital data of the anterior teeth uncovered by the splint and the arch were registered to define the relation between the trajectory and the condyle. The virtual simulation program was used to assess condylar movements. Finally, the protrusive condylar path and laterotrusive condylar path were obtained (Fig 6).

The accuracy of the trajectories is not evaluated here, as the chief purpose of this study regarding measurement of trajectory was to provide a calculation and visualization method for the motion path of the condyle.

RESULTS

The overall deviation of the 3D model data acquired by the PN-300 in combination with the model scanner was 12 ± 14 μm, and the RMS error (RMSE) was 27 ± 2.7 μm.

The distance deviations of relative linear movement trajectories (ΔD) are shown in Table 1. SPSS 19.0 statistical software (IBM) was used to analyze the data. Kolmogorov-Smirnov test showed that the deviation in movement distance of each axis was normally distributed, and Levene test showed that the data had a uniform variance. One-way analysis of variance was used to compare the movement distance deviation of the target on each axis, and least significant difference test was used to perform pairwise comparisons. The test level was bilateral, with $\alpha = .05$. The result was that the

distance deviations along the x and z axes had no statistical difference, and the deviations along these axes were both different from the y axis. The mean distances between the points of the relative movement trajectory and the fitted line were 82.7 ± 27.4 μm in total, 95.9 ± 8.6 μm along the x axis, 46.2 ± 6.4 μm along the y axis, and 106.1 ± 9.9 μm along the z axis. They all had a statistical difference.

The radius deviations of relative circular movement trajectories are shown in Table 2. Statistical analysis was the same as for analysis of linear movement. The data were normally distributed and had a uniform variance. The result was that the radius deviations along the xoy plane and yoz plane had no statistical difference, and the radius deviations along the xoy plane and yoz plane were different from the xoz plane. The mean distance of the points of relative movement trajectory to the fitted circle were 65.9 ± 10.6 μm in total, 56.5 ± 6 μm along the xoy plane, 77 ± 8 μm along the xoz plane, and 64.6 ± 5 μm along the yoz plane. They all had a statistical difference.

When the mandibular target made rectangular quadrilateral movements along the xoy, yoz, and xoz planes, the overall angle errors of the lines adjacent to the relative movement trajectory were 0.01 ± 0.1 degrees in total, 0.05 ± 0.1 degrees along the xoy plane, −0.04 ± 0.05 degrees along the xoz plane, and 0.03 ± 0.10 degrees along the yoz plane. The overall angle errors along the xoy plane and yoz plane had no statistical difference, and the overall angle errors along the xoy plane and yoz plane were different from the xoz plane, respectively.

The articulator simulated protrusive and laterotrusive movements. The mean deviation of the inclination of protrusive incisal guidance was 1.51 ± 0.68 degrees, and the inclination of laterotrusive incisal guidance was 0.82 ± 0.55 degrees. The results are shown in Tables 3 and 4. The result of a single-sample t test was that the angle error was statistically significant ($P < .05$) under each set point.

DISCUSSION

This study established a virtual articulator system based on binocular stereovision scanning and simulation technology. Unlike other existing mandibular movement recording systems, this system can obtain the mandibular movement relative to the maxilla without the need for complicated mechanical devices on the patient's head and can avoid the relative motions of the soft tissues. Considering the movements of the human jaw are composed of the movement of the head and neck and the mandible,[36] the system can simultaneously record the movement of the maxilla and mandible and then obtain the mandibular movement relative to the maxilla using a matrix transformation.

To simulate the mandibular movement, the mandibular movement data need to be integrated with the dental 3D data in the same coordinate system. Li et al[37] fused the spatial mandibular movement acquired by the ARCUSdigma and 3D digital model into one coordinate system via an occlusion fork, but this method required scanning the maxillary cast with the fork and manually establishing a coordinate system based on the fork, adding steps and sources of error. Koseki et al,[32] Fushima and Kobayashi,[38] He et al,[39] Baltali et al,[18] and Moriuchi et al[40] combined and merged 3D CBCT data and jaw-movement tracking data via spherical radiopaque markers. Low precision and gamma rays cannot be neglected. Kim et al[41] and Kwon et al[42] used a facial scanner to record the trajectory of mouth opening and closing as a digital movie to show real-time movement. The accuracy of a facial scanner is always unsatisfactory, and the price is not affordable for all hospitals. Nevertheless, the PN-300, which consists of two industrial cameras and a project module, can obtain the movement data and 3D data of anterior teeth in the same coordinate system simultaneously. 3D data of anterior teeth can be replaced by intraoral or cast scan data to detect occlusal contacts, as well as by CBCT data to visualize the movement of the TMJ during mandibular movement directly. Compared to other systems, it simplifies the operation and reduces the cost.

This experiment used an electronic translation stage to simulate the translational and rotational movements of the mandible for evaluating the system measurement accuracy. The results showed that the system has a larger error in the optical axis direction of the cameras; that is, the y axis. When the target moved in the direction of the optical axis of the cameras, the movement offset the instability of the system for identifying the

Table 1 Distance Deviations (μm) of Relative Linear Movement Trajectories Along the Three Axes

	x	y	z	Mean
a	−18 ± 7.7	2.4 ± 6.8	−15 ± 6.9	−10.2 ± 11.4
b	−19.2 ± 7	7.4 ± 11.7	−14.8 ± 6.9	−8.9 ± 14.6
c	−17.6 ± 7.5	4.2 ± 5.6	−15.6 ± 9	−9.7 ± 12.4
Mean	−18.3 ± 6.9[a]	4.7 ± 8.2[a,b]	−15.1 ± 7.1[b]	−9.6 ± 12.6

The same superscript lowercase letter shows a significant difference between groups. a, b, and c refer to the three centers of the concentric circles of the target. b = right angle vertex of the triangle; a = vertex in the same perpendicular direction as b; c = vertex in same horizontal direction as b.

Table 2 Radius Deviations (μm) of Relative Circular Movement Trajectories Along Three Planes

	xoy	xoz	yoz	Mean
a	13 ± 3.5	−22.6 ± 2.9	11.8 ± 2.3	0.7 ± 17.3
b	12 ± 2.3	−22.8 ± 3.1	12.4 ± 3.3	0.5 ± 17.3
c	13.8 ± 1.3	−20.8 ± 2.2	15 ± 3.7	2.7 ± 17.3
Mean	12.9 ± 2.5[a]	−22 ± 2.7[a,b]	13 ± 3.2[b]	1.3 ± 16.9

The same superscript lowercase letter shows a significant difference between groups. a, b, and c refer to the three centers of the concentric circles of the target. b = right angle vertex of the triangle; a = vertex in the same perpendicular direction as b; c = vertex in same horizontal direction as b.

Table 3 Mean Inclination of Protrusive Incisal Guidance Measured by PN-300 Under Different Set Inclinations

Inclination	0	10	20	30	40	
Mean	0.59	10.96	21.84	31.18	42.34	
SD	0.24	0.20	0.13	0.11	0.35	
Minimum	0.19	10.66	21.61	31.64	41.59	
Maximum	0.97	11.35	22.03	31.98	42.77	
Overall						1.51 ± 0.68

All data are reported in degrees. SD = standard deviation.

Table 4 Mean Inclination of Laterotrusive Incisal Guidance Measured by PN-300 Under Different Angle Parameters

Angle parameter	0	10	20	30	40	
Mean	0.45	10.59	20.80	30.75	42.07	
SD	0.17	0.19	0.13	0.14	0.20	
Minimum	0.25	10.33	10.55	30.56	41.67	
Maximum	0.75	10.97	10.96	30.95	42.32	
Overall						0.82 ± 0.55

All data are reported in degrees. SD = standard deviation.

center, resulting in minimal deviation. Sources of measurement error may include visual hardware, software, and the measurement environment, and these errors consist mainly of systematic errors and random errors. Structural errors were the main hardware errors, including the quantization error caused by the camera itself and its pixel resolution. Software errors were mainly the cumulative error caused by calibration, image processing, and matrix transformation.[43] The measurement environment (such as the light),

which is characterized by contingency, was the primary random error.

In this experiment, the PROTARevo7 articulator was used to simulate protrusive and laterotrusive movements of the mandible. When the sphere at the top of the incisal guide pin moved along the incisal guide table, the distance between the center of the sphere and the plane of the guide table was always the radius of the sphere so that the movement trajectories of the center were parallel with the table. Therefore, by calculating the angle between the trajectory of the sphere center and the horizontal plane, the accuracy of the inclination of incisal guidance derived from the PN-300 could be analyzed. The angle errors were bigger than simulated by the electronic translation stage. The reason may be that error sources also came from the FARO measurement system, registration process, and simulation process in addition to the sources mentioned above.

This experiment primarily quantitatively evaluated the accuracy of the PN-300 virtual articulator system using an electronic translation stage and an articulator. Compared to other systems and technologies mentioned, this self-developed virtual articulator system has a higher accuracy and stability. Moreover, a new method to calculate the condylar path was established. In the future, such a method may be used in the production of dental restorations as a dynamic virtual articulator for identifying eccentric premature occlusal contacts during mastication.[14,44,45] Further research is needed to detect occlusal contacts during mandibular movement to achieve dynamic occlusal adjustment and to determine the optimal position of the TMJ to perform oral rehabilitation and complete denture restoration.

CONCLUSIONS

In this study, a virtual articulator system, the PN-300, was proposed to record and simulate personalized mandibular movements and visualize the movement of the condyle. Laboratory evaluation was conducted. Deviations of known trajectories (straight line and circular arc) were below 100 μm, and the angle deviation of the rectangular quadrilateral plane was within 0.2 degrees, while the deviation of the inclination of incisal guidance was about 2 degrees. The PN-300 achieved a good accuracy for recording mandibular movement and can be expected to calculate the movement of the condyle.

ACKNOWLEDGMENTS

REFERENCES

1. Chang WS, Romberg E, Driscoll CF, Tabacco MJ. An in vitro evaluation of the reliability and validity of an electronic pantograph by testing with five different articulators. J Prosthet Dent 2004;92:83–89.
2. Chen CC, Lin CC, Chen YJ, Hong SW, Lu TW. A method for measuring three-dimensional mandibular kinematics in vivo using single-plane fluoroscopy. Dentomaxillofac Radiol 2013;42:95958184.
3. Gallo LM. Modeling of temporomandibular joint function using MRI and jaw-tracking technologies—Mechanics. Cells Tissues Organs 2005;180:54–68.
4. Fukui T, Tsuruta M, Murata K, Wakimoto Y, Tokiwa H, Kuwahara Y. Correlation between facial morphology, mouth opening ability, and condylar movement during opening-closing jaw movements in female adults with normal occlusion. Eur J Orthod 2002;24:327–336.
5. Pinheiro AP, Pereira AA, Andrade AO, Bellomo D. Measurement of jaw motion: The proposal of a simple and accurate method. J Med Eng Technol 2011;35:125–133.
6. Santos IC, Tavares JM, Mendes JG, Paulo MP. Acquisition and analysis of 3D mandibular movement using a device based on electromagnetic sensors and a neural network. J Med Eng Technol 2009;33:437–441.
7. Albuquerque LC, Silva HJ. Jaw movement in people with Parkinson's Disease. Codas 2016;28:193–196.
8. Fuentes R, Navarro P, Curiqueo A, Ottone NE. Determination of mandibular border and functional movement protocols using an electromagnetic articulograph (EMA). Int J Clin Exp Med 2015;8:19905–19916.
9. Solaberrieta E, Barrenetxea L, Minguez R, Iturrate M, De Prado I. Registration of mandibular movement for dental diagnosis, planning and treatment. Int J Interact Des Manuf 2018;12:1027–1038.
10. Fang J, Kuo T. Tracked motion-based dental occlusion surface estimation for crown restoration. Comput Aided Design 2009;41:315–323.
11. Maestre-Ferrín L, Romero-Millán J, Peñarrocha-Oltra D, Peñarrocha-Diago M. Virtual articulator for the analysis of dental occlusion: An update. Med Oral Patol Oral Cir Bucal 2012;17:e160–e163.
12. Koralakunte PR, Aljanakh M. The role of virtual articulator in prosthetic and restorative dentistry. J Clin Diagn Res 2014;8:ZE25–ZE28.
13. Ruge S, Quooss A, Kordass B. Variability of closing movements, dynamic occlusion, and occlusal contact patterns during mastication. Int J Comput Dent 2011;14:119–127.
14. Gärtner C, Kordass B. The virtual articulator: Development and evaluation. Int J Comput Dent 2003;6:11–24.
15. Solaberrieta EEOM. Virtual production of dental prostheses using a dentalvirtual articulator. Int J Interact Des Manuf 2015;9:19–30.
16. Han BJ, Kang H, Liu LK, Yi XZ, Li XQ. Comparisons of condylar movements with the functional occlusal clutch and tray clutch recording methods in CADIAX system. Int J Oral Sci 2010;2:208–214.
17. Farronato G, Giannini L, Galbiati G, Stabilini SA, Maspero C. Orthodontic-surgical treatment: Neuromuscular evaluation in open and deep skeletal bite patients. Prog Orthod 2013;14:41.
18. Baltali E, Zhao KD, Koff MF, Durmuş E, An KN, Keller EE. A method for quantifying condylar motion in patients with osteoarthritis using an electromagnetic tracking device and computed tomography imaging. J Oral Maxillofac Surg 2008;66:848–857.
19. Wieckiewicz M, Zietek M, Nowakowska D, Wieckiewicz W. Comparison of selected kinematic facebows applied to mandibular tracing. Biomed Res Int 2014;2014:818694.
20. Enciso R, Memon A, Fidaleo DA, Neumann U, Mah J. The virtual craniofacial patient: 3D jaw modeling and animation. Stud Health Technol Inform 2003;94:65–71.
21. Walczyńska-Dragon K, Baron S, Nitecka-Buchta A, Tkacz E. Correlation between TMD and cervical spine pain and mobility: Is the whole body balance TMJ related? Biomed Res Int 2014;2014:582414.
22. Kijak E, Lietz-Kijak D, Frączak B, Śliwiński Z, Margielewicz J. Assessment of the TMJ dysfunction using the computerized facebow analysis of selected parameters. Biomed Res Int 2015;2015:508069.
23. Hanssen N, Ruge S, Kordass B. SICAT function: Anatomical real-dynamic articulation by merging cone beam computed tomography and jaw motion tracking data. Int J Comput Dent 2014;17:65–74.
24. Al-Saleh MA, Punithakumar K, Lagravere M, et al. Three-dimensional morphological changes of the temporomandibular joint and functional effects after mandibulotomy. J Otolaryngol Head Neck Surg 2017;46:8.

25. Azuma T, Ito J, Kutsuki M, Nakai R, Fujita S, Tsutsumi S. Analysis of the mandibular movement by simultaneous multisection continuous ultrafast MRI. Magn Reson Imaging 2009;27:423–433.
26. Krohn S, Gersdorff N, Wassmann T, et al. Real-time MRI of the temporomandibular joint at 15 frames per second—A feasibility study. Eur J Radiol 2016;85:2225–2230.
27. Roeloffs V, Voit D, Frahm J. Spoiling without additional gradients: Radial FLASH MRI with randomized radiofrequency phases. Magn Reson Med 2016;75:2094–2099.
28. Furtado DA, Pereira AA, Andrade AO, Bellomo DP Jr, da Silva MR. A specialized motion capture system for real-time analysis of mandibular movements using infrared cameras. Biomed Eng Online 2013;12:17.
29. Zhao T, Yang H, Sui H, Salvi SS, Wang Y, Sun Y. Accuracy of a real-time, computerized, binocular, three-dimensional trajectory-tracking device for recording functional mandibular movements. PloS One 2016;11:e0163934.
30. Fang JJ, Kuo TH. Modelling of mandibular movement. Comput Biol Med 2008;38:1152–1162.
31. Xiaofeng Y, Huan QI. Calibration of binocular stereo-vision system based on ZHANG Zhengyou Plane Template Method. Mechanical Engineer 2014:1–3.
32. Koseki M, Niitsuma A, Inou N, Maki K. Three-dimensional display system of individual mandibular movement. In: Wu J, Fukuyama H, Ito K, Nishida T, Tobimatsu S (eds). Complex Medical Engineering. Tokyo: Springer, 2007:117–127.
33. Hu Z, Fei-peng DA, De-kui X. Algorithm of centre location of ellipse in optical measurement. J Applied Optics 2008;29:905-911.
34. Canny J. A computational approach to edge detection. IEEE Trans Pattern Anal Mach Intell 1986;8:679–698.
35. Tian S, Dai N, Cheng X, Li L, Sun Y, Cui H. Relative trajectory-driven virtual dynamic occlusal adjustment for dental restorations. Med Biol Eng Comput 2019;57:59–70.
36. Zafar H, Eriksson PO, Nordh E, Häggman-Henrikson B. Wireless opto-electronic recordings of mandibular and associated head-neck movements in man: A methodological study. J Oral Rehabil 2000;27:227–238.
37. Li HB, Wu GX, Zhang H, Feng HL, Li YS. The preliminary study of three-dimensional simulation of the craniofacial system. Zhonghua Kou Qiang Yi Xue Za Zhi 2005;40:405–407.
38. Fushima K, Kobayashi M. Mixed-reality simulation for orthognathic surgery. Maxillofac Plast Reconstr Surg 2016;38:13.
39. He S, Kau CH, Liao L, Kinderknecht K, Ow A, Saleh TA. The use of a dynamic real-time jaw tracking device and cone beam computed tomography simulation. Ann Maxillofac Surg 2016;6:113–119.
40. Moriuchi E, Hamanaka R, Koga Y, et al. Development and evaluation of a jaw-tracking system for mice: Reconstruction of three-dimensional movement trajectories on an arbitrary point on the mandible. Biomed Eng Online 2019;18:59.
41. Kim JE, Kwon JH, Kim JH, Shim JS. Recording the trajectory of mouth opening and closing for the fabrication of an occlusal splint. J Prosthet Dent 2017;117:597–600.
42. Kwon JH, Im S, Chang M, Kim JE, Shim JS. A digital approach to dynamic jaw tracking using a target tracking system and a structured-light three-dimensional scanner. J Prosthodont Res 2019;63:115–119.
43. Yang L, Wang B, Zhang R, Zhou H, Wang R. Analysis on location accuracy for the binocular stereo vision system. IEEE Photonics J 2018;10:1–16.
44. Röhrle O, Waddell JN, Foster KD, Saini H, Pullan AJ. Using a motion-capture system to record dynamic articulation for application in CAD/CAM software. J Prosthodont 2009;18:703–710.
45. Kordaß B, Gärtner C. The virtual articulator concept and development of VR-tools to analyse the dysfunction of dental occlusion. International Congress Series 2001;1230:689–694.

Literature Abstracts

Which Treatment Is Effective for Bruxism: Occlusal Splints or Botulinum Toxin?

The aim of the present study was to compare the efficacy of an occlusal splint and botulinum toxin for the treatment of bruxism. A total of 73 patients with myofascial pain due to bruxism were included in the present study. The patients were allocated into three groups: Group A was treated with an occlusal splint, group B with botulinum toxin injections, and group C with an occlusal splint and botulinum toxin injections. The Temporomandibular Disorder Pain Screener, Graded Chronic Pain Scale, Oral Behavior Checklist, Jaw Functional Limitation Scale, and visual analog scale (VAS) for pain on palpation of the chewing muscles were administered to all patients before treatment and 6 months after treatment. The questionnaire and VAS scores decreased in all three groups ($P < .0001$). The VAS and questionnaire scores were decreased significantly in groups B and C compared to those in group A (mean VAS score: group A = 5 [range 3 to 7]; group B = 1.9 ± 0.97; group C = 1.79 [range 0 to 3]). Occlusal splints might not be necessary for patients treated with botulinum toxin injections.

Occlusal Migration of Teeth Adjacent to Implant Prostheses in Adults: A Long-Term Study

To evaluate the effect of continuous tooth eruption on the outcomes of single-implant–supported restorations in the anterior maxilla of adults. A total of 76 patients (age 21 to 78 years) treated with single-implant–supported restorations in the esthetic zone were included. Radiographs obtained at crown placement and follow-up examinations from 1 to 15 years postloading were analyzed with regard to vertical incisal plane changes of the implant-supported crown relative to adjacent teeth. Infraocclusion increased over time by 0.08 ± 0.02 mm/year. Infraocclusion was more pronounced ($P = .04$) for delayed (0.09 mm/year) vs immediate implant placement (0.06 mm/year) and for younger vs older adults (0.0013 mm/year per additional year of age; $P = .014$). No statistically significant association between infraocclusion and sex, ethnicity, implant site, timing of implant temporization, surgical protocol, or type of restoration was found. Infraocclusion of single-implant–supported maxillary anterior restorations may result in esthetic concerns over time. Greater infraocclusion occurs in delayed implant placement and in younger individuals.